Available online at www.sciencedirect.com

SciVerse ScienceDirect

Ceramics International 38 (2012) 4237–4244

CERAMICS INTERNATIONAL

www.elsevier.com/locate/ceramint

Reaction and phases from monoclinic zirconia and calcium aluminate cement at high temperatures

Y.L. Bruni [a,b], L.B. Garrido [a,c], E.F. Aglietti [a,b,c,*]

[a] Centro de Tecnología de Recursos Minerales y Cerámica (CETMIC): (CIC-CONICET-CCT La Plata), Camino Centenario y 506, C.C.49 (B1897ZCA) M.B.Gonnet, Buenos Aires, Argentina

[b] Facultad de Ciencias Exactas - Universidad Nacional de La Plata, UNLP, Argentina

[c] CONICET, Buenos Aires, Argentina

Received 6 January 2012; received in revised form 29 January 2012; accepted 30 January 2012
Available online 9 February 2012

Abstract

Solid state reaction using m-ZrO_2 and high alumina cement as starting materials was studied. Various compositions containing different proportions of calcium aluminate cement (5–50 mol% CaO in ZrO_2) were reaction sintered at 1300–1500 °C. Crystalline phase formation and densification of Ca stabilized ZrO_2 composites was investigated by X-ray diffraction analysis, density and shrinkage measurements. Scanning electron microscopy (SEM) combined with energy dispersive X-ray spectroscopy was used to examine the microstructure. The main crystalline phases formed are related to the expected with the equilibrium phase diagram of the ZrO_2–CaO–Al_2O_3 system. Stabilized c-ZrO_2 is formed with the composition of $Ca_{0.15}Zr_{0.85}O_{1.85}$. The sintering of the mixtures leads to porous composites materials. Textural properties were analyzed considering the initial composition and the present crystalline phases.

Keywords: Ca stabilized zirconia; Aluminous cement; Reaction sintering

1. Introduction

Composites of the CaO–Al_2O_3–ZrO_2 system, particularly various of the high zirconia content, have a composition suitable to be used in refractory and pyrometallurgical applications due to desired good chemical inertness and corrosion resistance. However, the available data that provide information about CaO–Al_2O_3–ZrO_2 system is limited. The binary CaO–ZrO_2 solid solutions are the more studied and concentrate as a cubic phase c-ZrO_2. A ternary solid solution C_7A_3Z calcium aluminozirconate phase (C: CaO; A: Al_2O_3; Z: ZrO_2) which forms from the binary cubic CaO–ZrO_2 and alumina was reported. The C_7A_3Z is a compound that possesses bonding properties as a cement and was detected in samples sintered above 1200 °C [1].

Calcia has been used commercially to stabilize pure zirconia. For the calcium doped PSZ, CaO addition is in the range of 7.5–8.7 mol% in ZrO_2 and, for commercial alloys, 8.4 mol% (4.0 wt%) has been most common. [2]. Standard materials with partial stabilization contain approximately 5 mol% CaO while for full stabilization 20 mol% is required. Ca stabilized zirconia is specifically used as kiln furniture, setter plates for electronic industry, crucibles for melting noble metals, lining for the glass pipe and fiber industry [3]. ZrO_2-based electrolytes usually contain commercial CaO doped zirconia (10–16 mol%) [4].

Ca stabilized ZrO_2 material can be prepared from different processing routes [5–7]. Generally, ZrO_2 and calcia powders by solid state reaction at high temperature are widely used [8,9]. Ca stabilized ZrO_2 was synthesized from other calcium compounds such as CO_3Ca or dolomite by conventional and microwave sintering [10]. Sol gel route using a polymeric technique, with citrate process, co-precipitation of very reactive nitrate gels as well as nanoparticles of monoclinic zirconia and dolomite produced by high-energy ball-milling also provide useful precursors [11,12]. Zirconia–hydroxyapatite powders as precursors which were produced by a chemical-precipitation method, can be used for processing the Ca stabilized ZrO_2 composites [13]. In addition, Ca stabilized ZrO_2 can be prepared from mechanical alloying using high-energy ball-milling of pure ZrO_2 [14].

* Corresponding author.
E-mail address: eaglietti@cetmic.unlp.edu.ar (E.F. Aglietti).

0272-8842/$36.00
doi:10.1016/j.ceramint.2012.01.082

However, the high-temperature reactions proceeding in the mentioned system $CaO–Al_2O_3–ZrO_2$ starting from the mixture of zirconia and high alumina cement (HAC) as precursors have not yet investigated.

Commercial HAC are pure materials with high melting point, which contains calcium aluminates (CA and CA_2) as principal crystalline phases accompanied by scarce α-Al_2O_3 and $C_{12}A_7$ [15]. Also HAC presents a relative low particle size that allows to be sintered or reacted with other compounds. Previous works reported the in situ formation of mullite–ZrO_2 composites through bauxite and alumina castables containing low HAC and zircon and studied their refractory properties [16]. Similarly the development of t-ZrO_2, besides spinel, periclase and CaO, MgO-silicate glassy phases, from a mixture of magnesite aggregates, fine zircon sand and high alumina refractory cement by sintering at 1550 °C have been reported [17]. Furthermore, the HAC commonly acts as bonding phase of alumina-magnesia castables and therefore, the in situ spinel ($MgAl_2O_4$), and the CA_2 and CA_6 formation at temperatures above 1200 °C was examined in detail [18]. Recently, the effect of HAC and hydratable alumina on the general castables properties of such spinel-containing alumina-based refractory castables was reviewed [19].

In this work, the formation of Ca stabilized ZrO_2 material with potential applications in filtration/separation processes from pure ZrO_2 containing different proportions of calcium aluminate cement (5–50 mol% CaO in ZrO_2) was investigated. Thus, CaO was introduced in the form of high alumina cement, and the effect of important factors such as chemical composition, sintering temperature on reaction, densification and microstructure was examined. In this case, the combination of HAC with pure ZrO_2 at high temperatures leads to phases in agreement with the $ZrO_2–CaO–Al_2O_3$ system. Most of the previous studies, as already mentioned, described the synthesis the calcium stabilized ZrO_2 composites from different raw materials but not from ZrO_2 and HAC.

2. Experimental procedure

2.1. Materials

Pure zirconia (m-ZrO_2) of commercial grade with a mean particle size d_{50} =8 μm was employed as reactant. Particle size distribution is narrow with particle sizes in a range of d_{90} = 15 μm and d_{10} = 5 μm. A commercial high alumina cement (HAC) used in the refractory industry was used as second reactive (Secar 71, Kerneos, France). Table 1 shows the main chemical composition of this raw material which was obtained from the product data sheet.

The mineralogical composition of HAC was verified using DRX indicating that the major components are monocalcium aluminate (CA), with monocalcium dialuminate (CA_2) 25% and scarce amounts of Al_2O_3.

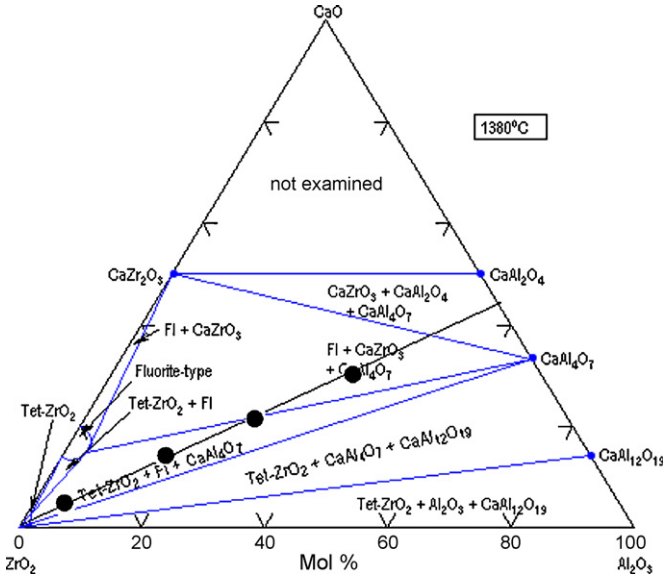

Fig. 1. Phase diagram of the $CaO–ZrO_2–Al_2O_3$ system. Isothermal section at 1380 °C from Muromura and Hinatsu [20]. Composition line corresponds to the initial compositions studied in this work.

Previous study reported that HAC shows specific surface area of 1.2 m^2/g and a wide particle size distribution containing particles sizes varying between 63 and 1 μm with a d_{50} = 13 μm [18].

From these two raw materials a series of mixtures of different chemical composition were prepared varying between 5 and 50 mol% of CaO in ZrO_2. Fig. 1 shows the phase diagram of the $CaO–ZrO_2–Al_2O_3$ system and the composition line corresponding to the initial compositions of this study [20].

The compacts were identified according to the CaO molar content respect to ZrO_2: 5, 15, 30 and 50 mol% of CaO and were named as: ZrC5, ZrC15, ZrC30 and ZrC50. The cylinders with a diameter of 30 mm and a height of near 5 mm, were obtained using uniaxial pressing (20 MPa). Reaction sintering was made with an electric furnace (Si_2Mo) in air atmosphere at different temperatures (1300–1500 °C) using a heating and cooling rate of 5 °C/min. The soaking time was of 2 h.

2.2. Characterization methods

Formed crystalline phases were analyzed by X-ray diffraction (XRD) (Philips 3020 equipment with Cu-Kα radiation in Ni filter at 40 kV–20 mA). The samples were analyzed in powder form. The relative content of cubic zirconia (c-ZrO_2) was determined from diffractograms using the semiquantitative method [21] for stabilized and m-ZrO_2 mixtures. This method employs the relation between the integrated areas of the

Table 1
Chemical composition of high alumina cement used.

HAC	Al_2O_3 (wt%)	CaO (wt%)	Na_2O (wt%)	SiO_2 (wt%)	Fe_2O_3 (wt%)	TiO_2 (wt%)
	68	30	0.5	0.2–0.6	0.1–0.2	0–0.4

diffraction peaks of the polymorphs of zirconia in the 27–33° 2θ range.

The relative density RD of composites (% of theoretical density TD) was determined from the ratio between the apparent density geometrically measured and theoretical density. Theoretical density of composite was calculated by the volume fraction of different phases obtained by DRX results and each phase density. The XRD analysis showed that initial phase composition changed after sintering. As will be discussed below, the main transformations were the formation of c-ZrO_2, decomposition of high alumina cement in CA_2 and CaO and formation of $CaZrO_3$. The CA_2 and CA densities were 3.1 and 2.91 g cm^{-3}, respectively. The transformation of m-ZrO_2 to cubic phase slightly reduced the density from 6 to 5.6 g cm^{-3}, respectively [4]. The $CaZrO_3$ (ZC) density is close to 4.62 g cm^{-3}. For simplicity, the approach followed to estimate the final phase composition was made assuming that added alumina took part of CA_2. The semi-quantitative method showed that maximum ZC content was near to 10–15 wt%. Finally, the TD was calculated and it resulted practically independent on the sintering temperature.

Linear shrinkage (radial) of composites was geometrically determined as a function of the sintering temperature. Porosity and the most frequent pore radius of the ZrC5–50 composites were measured using the Hg porosimeter Carlo Erba 2000, Italy.

Microstructure of the materials was observed using SEM (Quanta 200 FEI MK2 Serie) and microanalysis (MEB-EDX).

3. Results

3.1. Influence of sintering temperature and CaO content on phase formation

Figs. 2–6 show the XRD patterns of the compacts, ZrC5, ZrC15, ZrC30 and ZrC50 sintered at different temperatures.

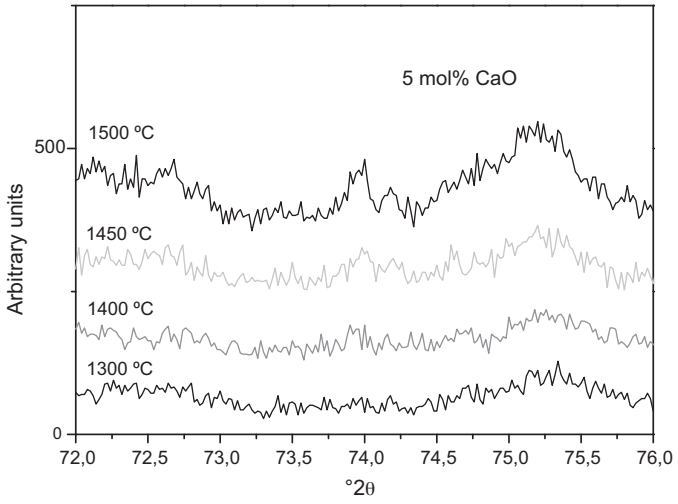

Fig. 3. XRD of the 72–76° 2θ region for ceramics with 5 mol% CaO in ZrO_2 sintered at different temperatures.

Fig. 2 shows the superpose diffractograms of ZrC5 at different temperatures. At 1300 °C the main crystalline phase was m-ZrO_2, accompanied with a low content of tetragonal (t-ZrO_2) and/or cubic zirconia (c-ZrO_2). The analysis of the principal reflections along the 25–32° 2θ degree (zone of the more intense peaks of ZrO_2 polymorphs) indicated the presence of t/c-ZrO_2. Small peaks of CA_2 were also present.

The CA and alumina phases were not detected in this composition at 1300 °C.

With the aim to establish if the stabilized zirconia was tetragonal or cubic, the 70–80° 2θ of the diffraction region was analyzed. In the region of 73–74.5° 2θ, the peak planes (4 0 0) for cubic and tetragonal ZrO_2 and that of (2 2 0) for the tetragonal phase appeared [10]. Fig. 3 showed the expanded diffraction zone for ZrC5 sintered at different temperatures. Peaks are of low intensity and definition, but the reflection centred at 73.8° 2θ for sample sintered at 1500 °C was indicative of the presence of c-ZrO_2.

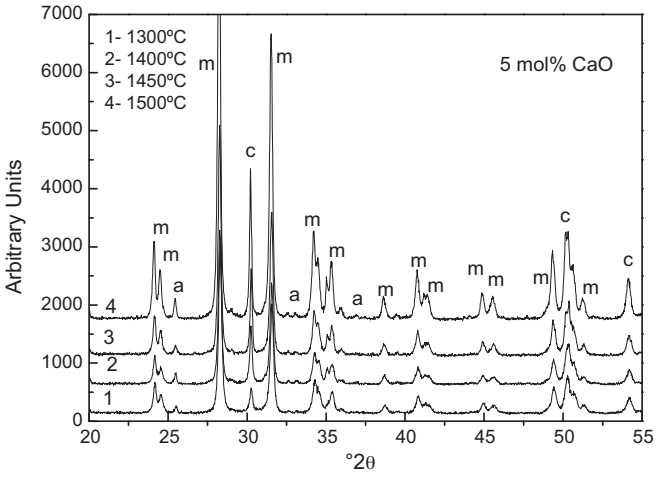

Fig. 2. XRD patterns of ceramics with 5 mol% CaO in ZrO_2 sintered at different temperatures (m: m-ZrO_2; c: c-ZrO_2; a: $CaAl_4O_7$; z: $CaZrO_3$; b: $CaAlO_4$).

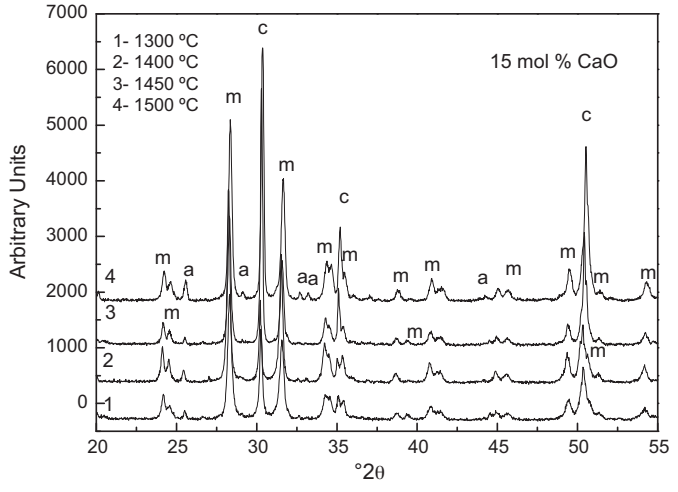

Fig. 4. XRD patterns of ceramics with 15 mol% CaO in ZrO_2 sintered at different temperatures (m: m-ZrO_2; c: c-ZrO_2; a: $CaAl_4O_7$; z: $CaZrO_3$; b: $CaAlO_4$).

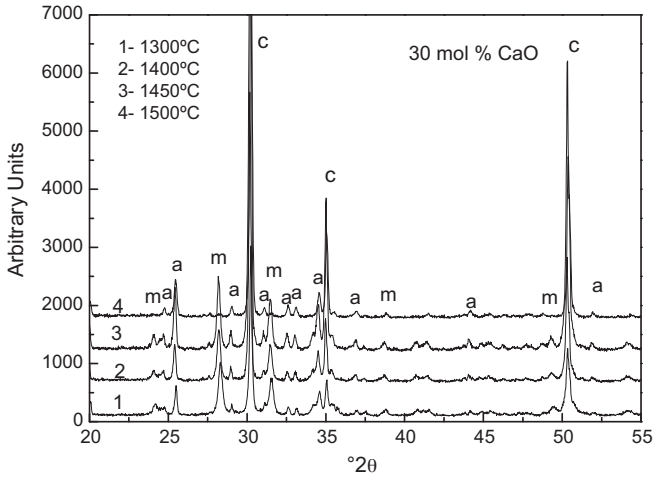

Fig. 5. XRD patterns of ceramics with 30 mol% CaO in ZrO_2 sintered at different temperatures (m: m-ZrO_2; c: c-ZrO_2; a: $CaAl_4O_7$; z: $CaZrO_3$; b: $CaAlO_4$).

With increasing sintering temperature at 1400 °C, more intense m-ZrO_2 peaks were found, probably due to the high crystallinity of this phase after the thermal treatment. This fact may be related to a crystal size growth at high temperatures. Also a relatively low increase in the CA_2 content, and in c-ZrO_2 formation occurred. Free alumina was not detected.

For the sintered ZrC15 (Fig. 4) a significant increase in the c-ZrO_2 content was observed in comparison with that of the 5 mol% composition. Besides the m-ZrO_2 content was important. The c-ZrO_2 increased from 1300 to 1500 °C, and a more crystallinity of m-ZrO_2 was observed. The relative content of CA_2 was related with c-ZrO_2 formation, so both phases had more intense reflections up to 1500 °C.

When the addition of CaO was 30 mol% (ZrC30) the c-ZrO_2 formation was favored even at 1300 °C (Fig. 5). With further increase in temperature (1300–1500 °C) an increase of CA_2 and a decrease in the m-ZrO_2 content were observed. The high formation of c-ZrO_2 at 1500 °C, was accompanied with an increase of m-ZrO_2 crystallinity. In this material sintered at 1500 °C., the characteristic peaks of calcium zirconate were detected. $CaZrO_3$ formation indicated that the equilibrium state was not reached because it is not an equilibrium phase for this composition (Fig. 1).

Diffractograms of ZrC50 sintered at different temperatures are shown in Fig. 6. The principal phases at 1300 °C were c-ZrO_2 and CA_2 with scarce m-ZrO_2. At this temperature, weak peaks of CA (unreacted) and $CaZrO_3$ were detected. At 1500 °C, ZrO_2 appeared as c-ZrO_2, while a relative reduction in the content of CA_2 was accompanied by formation of $CaZrO_3$.

The disappearance of CA and the absence of alumina can be explained by the following reactions:

$$2x\mathrm{CaO}\cdot\mathrm{Al_2O_3} + y\mathrm{ZrO_2} \rightarrow y\mathrm{ZrO_2(CaO)}_x + x\mathrm{CaO}\cdot\mathrm{Al_4O_6}$$

$$2x\mathrm{CA} + y\mathrm{Z} \rightarrow y\mathrm{Z(C)}_x + x\mathrm{CA_2}$$

3.2. Effect of CaO addition on c-ZrO_2 formation

XRD results indicated that during sintering, calcium coming from calcium aluminates decomposition, reacts with zirconia forming a solid solution with cubic structure. The c-ZrO_2 formation depended on CaO concentration and the sintering temperature.

Fig. 7 shows the evolution of c-ZrO_2 content with CaO addition and temperature. The relative proportion of c-ZrO_2 was determined using the Garvie–Nicholson method [21]. The c-ZrO_2 content of the ZrC5 composite sintered between 1300 and 1450 °C ranged between 5.6% and 16% respectively while that of the ZrC30 material increased from 50 to 97 by heating at the same temperatures. Thus, at low CaO additions (5–10%) the m-ZrO_2 was the principal phase and the sintering temperature slightly influenced the c-ZrO_2 formation. For the ZrC15 and ZrC30 compositions, c-ZrO_2 strongly increased from 50% at 1300 °C to 100% at 1500 °C and therefore, sintering

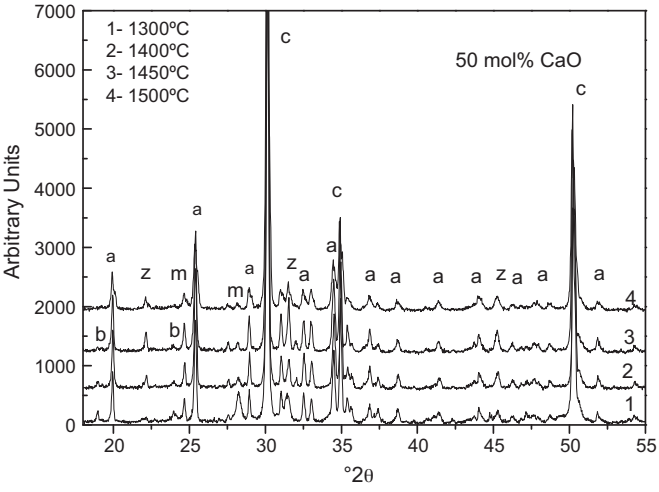

Fig. 6. XRD patterns of ceramics with 50 mol% CaO in ZrO_2 sintered at different temperatures (m: m-ZrO_2; c: c-ZrO_2; a: $CaAl_4O_7$; z: $CaZrO_3$; b: $CaAlO_4$).

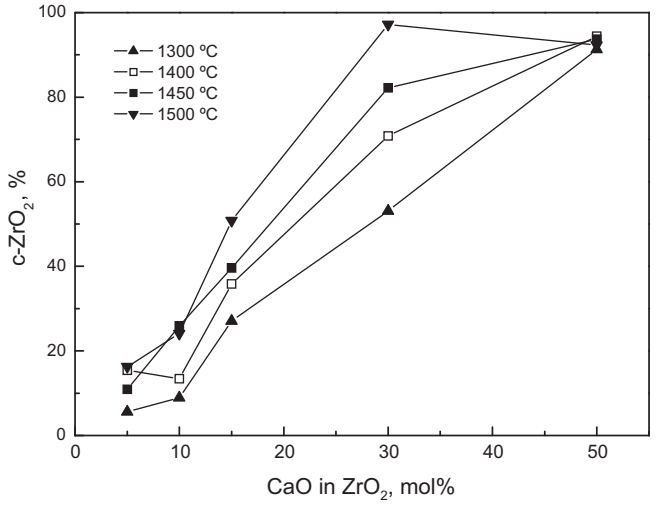

Fig. 7. Effect of CaO addition and sintering temperature on c-ZrO_2 formation.

temperature seems to be the principal processing parameter on c-ZrO_2 formation.

The transformation to c-ZrO2 was nearly complete at all temperatures for the ZrC50 sample. The CaO content was sufficient and enabled to obtain the c-ZrO_2 and $CaZrO_3$. In this sample the formation c-ZrO_2 was not affected by sintering temperature.

3.3. Experimental crystalline phases formed (XRD) related with equilibrium phase diagram

Fig. 1 shows the equilibrium phase diagram of the ZrO_2–CaO–Al_2O_3 system (isotherm at 1380 °C) [20] near a mean sintering temperature employed in this work. In this figure the composition line was also draw for the compositions studied. Along the composition line is possible to estimate the content of the different equilibrium phase that can be formed in our system. The estimation of crystalline phase content was performed using the phase diagram of the CaO–Al_2O_3–ZrO_2 system (Fig. 1) and was included in Table 2.

The phase diagram of the CaO–Al_2O_3–ZrO_2 system was first reported by Berezhnoi and Kordyuk [22]. They determined a single-phase region of the liquid and the stoichiometric composition of a ternary compound as $Ca_7A_{l6}ZrO_{18}$ (C_7A_3Z) with a melting point 1550 °C. Espinosa and White [23] however reported that the ternary compound is $Ca_{13}Al_{12}Zr_2O_{35}$ ($C_{13}A_6Z_2$) and that it decomposes into $CaZrO_3$ (CZ) plus liquid by a peritectic reaction at 1540 °C, this compound appears for high CaO content and establish a compatibily triangle CZ–$C_{13}A_6Z_2$–C [20,24].

An eutectoid decomposition reaction in the system ZrO_2–CaO, takes place between c-ZrO_2 and $CaZrO_3$ at the equilibrium temperature of 1140 °C forming a c-ZrO_2 solid solution with a 17 mol% of CaO and $C_6Zr_{19}O_{44}$ phase [25,26], but this phase did not appear in our samples.

The evolution of the crystalline phases observed in the four compositions studied was near to the expected ones by the equilibrium diagram (Fig. 1). The $CaZrO_3$ appeared in ZrC30 and ZrC50 materials treated at 1500 °C. According to the phase diagram of Fig. 1 the $CaZrO_3$ would be only formed in ZrC50 sample and in very low content. Also for ZrC50, no m-ZrO_2 would be present but a scarce content was detected in our sample. The content of $CaZrO_3$ was near to 13% for the ZrC50 material. For samples sintered at 1400 °C, the maximum content of c-ZrO_2 predicted was 62%.

Table 2
Crystalline phase contents (mole %) according to the equilibrium phase diagram at 1380 °C (Fig. 1).

Sample	m-ZrO_2	c-ZrO_2	CA_2	$CaZrO_3$
5	79	13	8	–
10	58	28	14	–
15	44	36	20	–
30	–	62	38	–
50	–	30	57	13

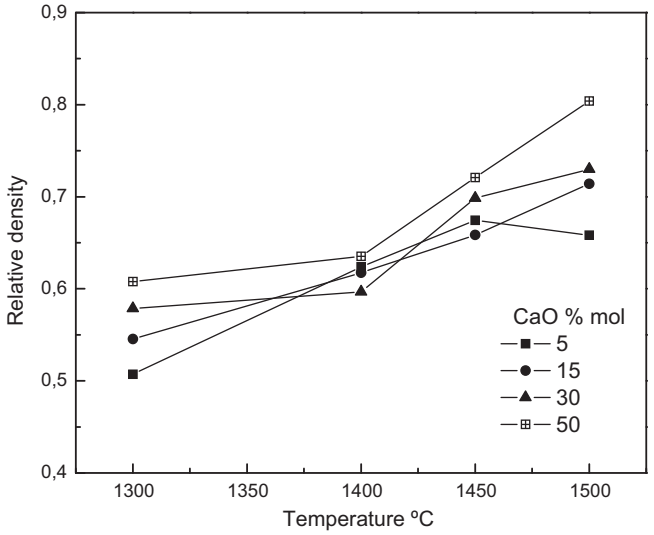

Fig. 8. Relative density RD of composites with 5–50 mol% CaO in ZrO_2 vs. sintering temperatures.

3.4. Sintering and microstructure of ZrC5–50 composites

Variation of relative density RD and shrinkage of ZrC5–50 compacts with sintering temperatures are shown in Figs. 8 and 9 respectively. The RD dependence on the sintering temperature slightly varied with chemical composition.

The RD of all materials sintered at 1300 °C remained lower than 0.6. These values were similar to the respective RD of the dried compacts which ranged between 0.50 and 0.58 with increasing CaO in the composition. The volume fraction of ZrO_2 in the starting powder compositions reduced from 0.846 to 0.25 for ZrC5 and ZrC50 mixtures, respectively. In the case of ZrC50 composition, the ZrO_2 content acting as a fine powder was closer to the optimum volume fraction of 0.29 for which the maximum packing density of solids in a binary powder mixtures occurs. Thus, this specific amount of ZrO_2 probably

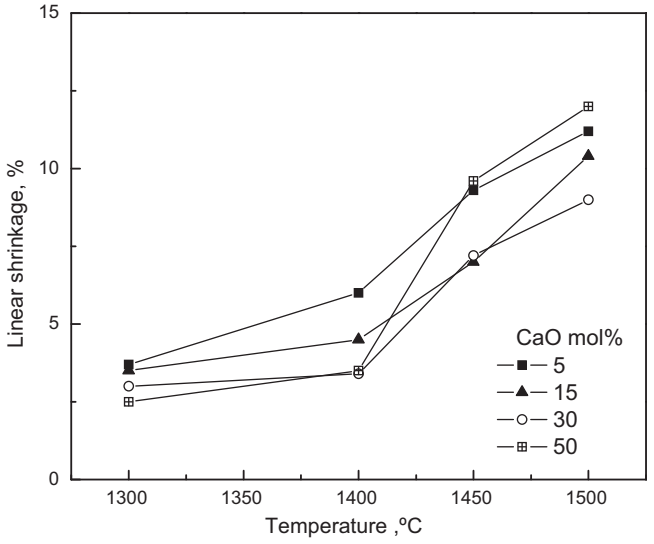

Fig. 9. Linear sintered shrinkage of ceramics vs. sintering temperatures for different mole % CaO in ZrO_2.

contributed to obtain a more efficient packing of solids in the dried compact.

The RD of ZrC5–15 compacts significantly increased from 0.50 at 1300 °C to 0.65 at 1450 °C, respectively and then, a further increase to 1500 °C only produced a minor change in densification. The RD of ZrC30 sample achieved up to 0.70 by sintering at 1450 °C which was a similar densification degree than that observed for 50 mol% materials. The ZrC50 composite reached high RD at a relative low sintering temperature than the materials produced from the compositions with lower content of CaO. In this case, the denser composite (RD = 0.78) was produced by sintering at 1500 °C. Therefore, densification slightly increased with increasing the content of HAC in the starting composition. Nevertheless, the pore volume fraction of all composites remained near to 0.4 at 1400 °C.

Fig. 9 shows the linear shrinkage vs sintering temperature curves for the ZrC5 to 50 composites. There are small differences in shrinkage between samples sintered at 1300 °C. The shrinkage varied between 4% and 2% for ZrC5 to ZrC50, respectively indicating the initial sintering condition. Shrinkage of ZrC5 and ZrC15 composites sintered at 1400 °C reached 6% that agreed well with the increase in densification. The increase in the sintering temperature promoted the neck formation which is associated to a reduction in porosity. Whereas shrinkage remained nearly constant to 3% for the higher CaO additions (RD resulted similar to that sintered at 1300 °C). The relatively lower shrinkage of samples containing 30–50 mol% CaO up to 1400 °C may be explained by the high RD of dried compact. Sintering at 1400–1450 °C caused a less pronounced increase in shrinkage of ZrC5 and ZrC15 in comparison with that corresponding to ZrC30 and ZrC50. There was a minor increase in densification observed for ZrC5 and ZrC15 at 1500 °C. Contrarily, high shrinkage of ZrC50 at 1500 °C was accompanied by high RD due to elimination and/or coalescence of small of pores.

Comparatively, the ZrC5 and ZrC15 compositions with high ZrO_2 content consolidated by dry pressing in a low packing density of solids (low dried RD) and consequently, a slightly lower RD resulted even after sintering at 1500 °C. The high ZrO_2 content and low packing density of particles inhibited full densification and resulted a high pore volume at 1500 °C. Pores consisted of interparticle voids coming from a non uniform packing of ZrO_2 aggregates. Contrarily, high proportion of HAC resulted in a wider particle size distribution in which finer particles fill the interstices left between coarse HAC particles. Therefore, a slight increase of the solid packing density of the dried compact was observed. In addition, formation of a liquid phase possibly occurred when temperature approximated to 1450 °C and caused the significant shrinkage and the improvements in densification of ZrC50 composite.

Figs. 10 and 11 show the SEM micrographs of the typical agglomerated microstructures of composites. The fine aggregates and coarse particles present in the starting ZrO_2 and HAC powders, respectively remained in the sintered composite. Light and gray color areas that appeared in the complex microstructure corresponds to ZrO_2 and CA_2 phases (identified by EDX), respectively. Composites contained significant

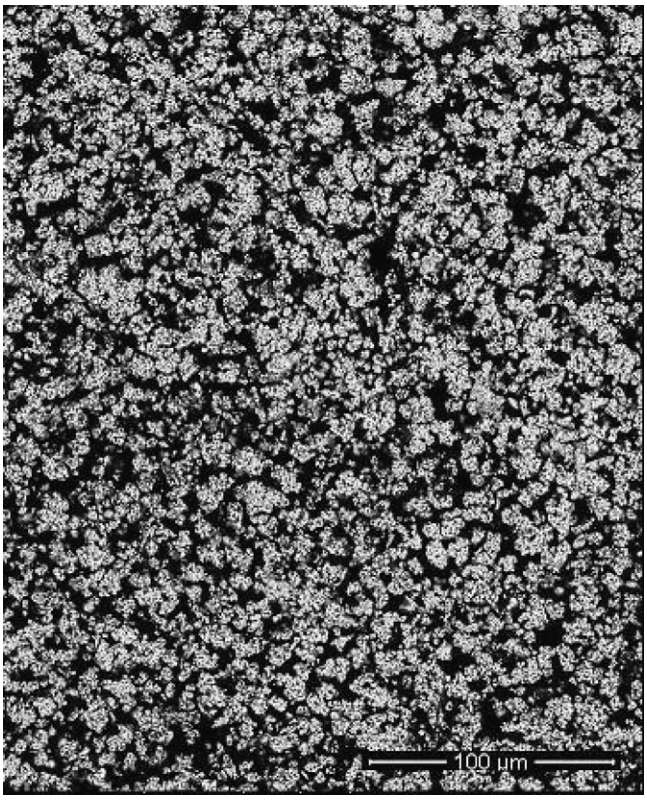

Fig. 10. SEM micrograph of composites with 5 mol% of CaO sintered at 1400 °C.

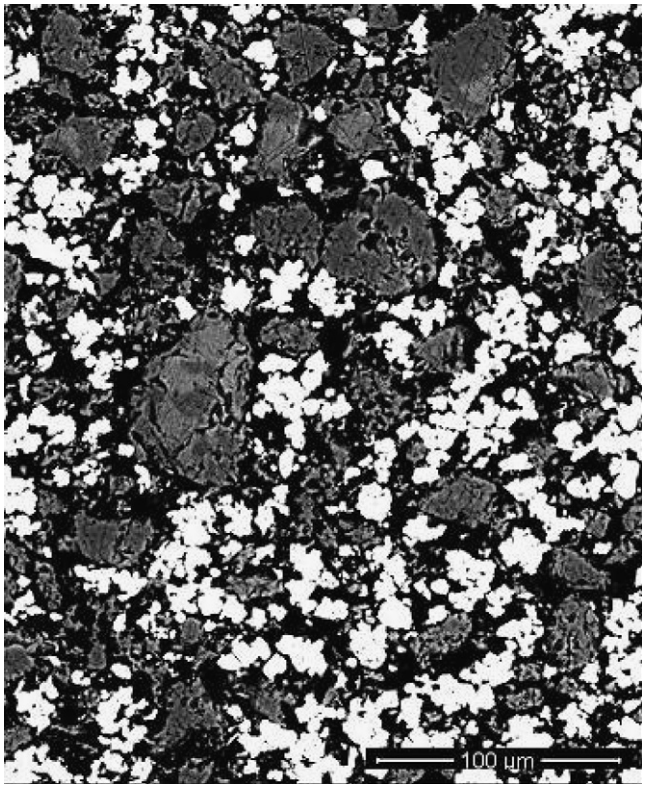

Fig. 11. SEM micrograph of composites with 50 mol% of CaO sintered at 1400 °C.

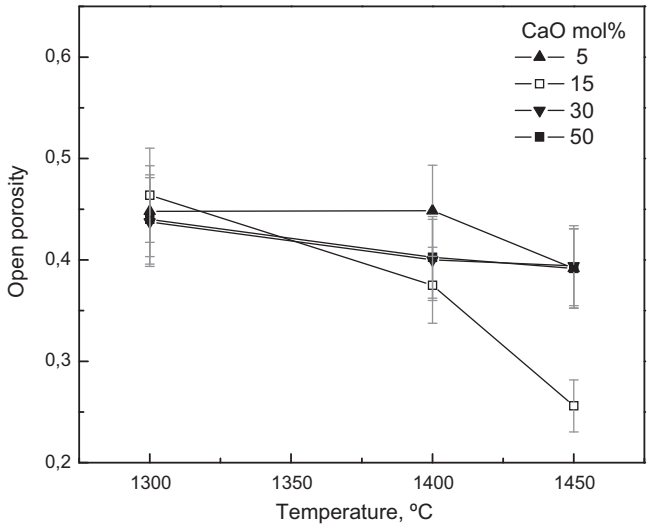

Fig. 12. Open porosity by Hg porosimetry vs. temperature for different mole %CaO content.

amount of pores (in dark color) as sintering of highly aggregated powder provided a highly porous ceramic.

Fig. 12 shows the evolution of open porosity (evaluated by Hg intrusion measurements) with increasing sintering temperatures. The data show a reduction of porosity with sintering temperature, as expected, but large deviations existed; then in Fig. 13 a clear trend of open porosity with the chemical composition was not observed. However, Hg porosimetry results supported the low densification degree obtained at 1400 °C.

On the other hand, the dependence of mean pore radius of ceramics (measured by Hg porosimetry) with sintering temperature varied with the starting powder composition. All samples exhibited a monomodal pore size distribution which was composed by pores having the characteristic radius near to 1 μm. Mean pore size for ZrC5 and ZrC15 ceramics reduced up to 0.8 μm at 1450 °C as sintering progressed. However, an opposite effect of sintering temperature was observed for the ZrC30 composites for which the mean pore radius attained 1.3 μm. Also, the ZrC50 composites exhibited an increase in most frequent pore radius from 1.25 μm for 1300 °C to 1.53 μm for 1450 °C, respectively.

Thus, porosity and mean pore size of composites which are important parameters for filtration applications remained suitable to develop an open pore structure.

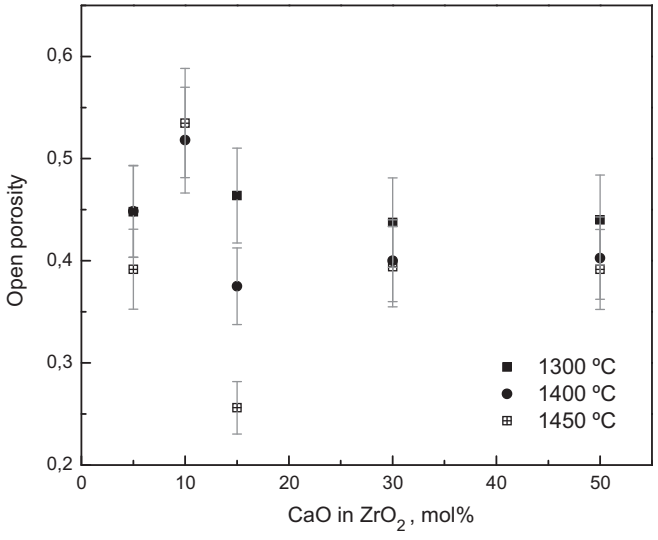

Fig. 13. Open porosity by Hg porosimetry vs. mole % CaO for different temperatures.

4. Conclusions

Sintering of mixtures of m-ZrO_2 with high alumina cement HAC as a source of CaO at 1300–1500 °C was effective to produce porous Ca stabilized ZrO_2 composites.

DRX results indicated that during sintering, calcium coming from calcium aluminates decomposition, reacts with zirconia forming a solid solution with cubic structure (c-ZrO_2, $Ca_{0.15}Zr_{0.85}O_{1.85}$). The c-$ZrO_2$ formation depended on CaO concentration and the sintering temperature. The ceramics containing 5–15 mol% CaO sintered up to 1500° C are composed by a combination of monoclinic and c-ZrO_2 phases with a low proportion of calcium dialuminate CA_2 ($CaAl_4O_7$). The stabilization was partial and the m-ZrO_2 predominated.

The sintering temperature slightly influenced the c-ZrO_2 formation at low CaO additions (5–10 mol%). For the ZrC15 and ZrC30 composites, c-ZrO_2 strongly increased from 50% at 1300 °C to 100% at 1500 °C and consequently, sintering temperature seems to be the principal processing parameter on c-ZrO_2 formation. The maximum conversion to $Ca_{0.15}Zr_{0.85}O_{1.85}$ was observed for 30 mol% at 1450 °C.

The transformation to c-ZrO_2 for the ZrC50 sample was nearly complete by sintering even at 1300 °C. The formed phases are close to those predicted by the equilibrium phase diagram.

The high ZrO_2 content and the narrow particle size distribution of ZrC5 and ZrC15 conducted to inhomogeneous and less dense particle packing in the compact resulting a comparatively low mean pore size. Contrarily, the presence of high proportion of HAC for ZrC50 provided a relatively denser powder packing in the dried compact which favored contact between particles, and consequently enhanced the sintering process. The densification gradually increased with temperature and is improved at 1500 °C. However the reduction in pore volume occurred approximating to 1400 °C and it was accompanied by a significant increase in the mean pore size of the composite.

Nevertheless, open porosity and mean pore size of composites remained suitable to develop an open pore structure with potential for filtration applications.

References

[1] V.D. Barbanyagre, D.A. Mishin, Synthesis and some properties of a new compound in the CaO–Al_2O_3–ZrO_2 system, Refract. Ind. Ceram. 41 (2000) 356–359.

[2] R.H.J. Hannink, Transformation toughening in zirconia-containing ceramics, J. Am. Ceram. Soc. 83 (2000) 461–487.

[3] H.H. Zender, H. Leistner, H. Searle, ZrO_2 materials for application in the ceramics industry, Interceramics 39 (1990) 33–38.
[4] R. Muccillo, R.C. Buissa Netto, E.N.S. Muccillo, Synthesis and characterization of calcia fully stabilized zirconia solid electrolytes, Mater. Lett. 49 (2001) 197–201.
[5] A.K. Shukla, V. Sharma, N. Arul Dhas, K.C. Patil, Oxide-ion conductivity of calcia- and yttria-stabilized zirconias prepared by a rapid-combustion route, Mater. Sci. Eng. B 40 (1996) 153–157.
[6] M.E. Contreras-Garcıá, I. Espitia-Cabrera, J. Serrato-Rodrıguez, J. Reyes-Gasga, Synthesis and processing of Ca-PSZ pellets by a spray-drying method, Mater. Res. Bull. 35 (2000) 1171–1186.
[7] C. Lin, X. Zhang, Y. Hou, Y. Wang, G. Wang, Synthesis of calcium oxide stabilized cubic zirconia powders by electrochemical method, Adv. Mater. Res. 233–235 (2011) 2403–2408.
[8] K. Haberko, W. Pyda, Preparation of Ca-stabilized ZrO_2 micropowders by a hydrothermal method, in: N. Claussen, M. Rühle, A.H. Heuer (Eds.), Advances in Ceramics V. 12, Science and Technology of Zirconia II, ACS, Columbus, OH, 1984, pp. 774–783.
[9] S.K. Durrani, J. Akhtar, M. Ahmad, M.A. Hussain, Synthesis and characterization of low density calcia stabilized zirconia ceramic for high temperature furnace application, Mater. Chem. Phys. 100 (2006) 324–328.
[10] S. Nath, N. Sinha, B. Basu, Microstructure, mechanical and tribological properties of microwave sintered calcia-doped zirconia for biomedical applications, Ceram. Int. 34 (2008) 1509–1520.
[11] E. Mustafá, Ca-PSZ prepared via polymeric sol–gel route, Ceram. Int. 26 (2000) 215–220.
[12] J. Carretero, M.A. Sainz, S. Serena, A. Caballero, Obtención de circonas estabilizadas (Ca,Mg-PSZ) nanocristalinas a partir de mezclas de dolomita y circona monoclínica mediante molienda de alta energía, Bol. Soc. Esp. Cerám. Vidrio 42 (2003) 303–310.
[13] V. Silva, F. Soares Lameirasa, R. Zacarias Domingues, Synthesis and characterization of calcia partially stabilized zirconia-hydroxyapatite powders prepared by co-precipitation method, Ceram. Int. 27 (2001) 615–620.
[14] D. Michel, F. Faudot, E. Gaffet, L. Mazerolles, Stabilized zirconias prepared by mechanical alloying, J. Am. Ceram. Soc. 76 (1993) 2884–2888.
[15] K.M. Parker, J.H. Sharp, Refractory calcium aluminate cements, Trans. J. Br. Ceram. Soc. 81 (1982) 35–42.
[16] M.F. Zawrah, Effect of zircon additions on low and ultra-low cement alumina and bauxite castables, Ceram. Int. 33 (2007) 751–759.
[17] M. Awaad, A.G.M. Othman, Characterization and evaluation of some low-cement zircon-magnesia refractory concretes, Ind. Ceram. 26 (2006) 203–208.
[18] M.A.L. Braulio, G.G. Morbioli, D.H. Milanez, V.C. Pandolfelli, Calcium aluminate cement source evaluation for Al_2O_3–MgO refractory castables, Ceram. Int. 37 (2011) 215–221.
[19] M.A.L. Braulio, M. Rigaud, A. Buhr, C.D. Parr, V.C. Pandolfelli, Spinel-containing alumina-based refractory castables, Ceram. Int. 37 (2011) 1705–1724.
[20] T. Muromura, Y. Hinatsu, Phase relation of ternary system ZrO_2–CaO–Al_2O_3, Mater. Res. Bull. 21 (1986) 61–67.
[21] R. Garvie, P.S Nicholson, Phase analysis in zirconia systems, J. Am. Ceram. Soc. 55 (1972) 303–305.
[22] S. Berezhnoi, R.A. Kordyuk, Dokl. Akad. Nauk USSR 10 (1963) 1334.
[23] J. Espinosa, J. White, Compatibility relationships in the system ZrO_2–Al_2O_3–CaO, Bol. Soc. Esp. Ceram. Vidrio 12 (1973) 237.
[24] T. Murakami, H. Fukuyama, T. Kishida, M. Susa, K. Nagata, Phase diagram for the system ZrO_2–Al_2O_3–CaO, Metall. Mater. Trans. B 31b (2000) 25–33.
[25] J.R. Hellmann, V.S. Stubican, Stable and metastable phase relations in the system ZrO_2–CaO, J. Am. Ceram. Soc. 66 (2) (1983) 260–264.
[26] V.S. Stubican, G.S. Corman, J.R. Hellmann, G. Senft, Phase relationships in some ZrO_2 systems, Adv. Ceram. Sci. Technol. Zirconia II 12 (1984) 96–106.